Author Manuscript

Author Manuscript

Author Manuscript

Author Manuscript

HHS Public Access

Author manuscript

Mol Cancer Ther. Author manuscript; available in PMC 2020 June 01.

Published in final edited form as:

Mol Cancer Ther. 2019 June ; 18(6): 1127–1136. doi:10.1158/1535-7163.MCT-18-0953.

Enhancing Therapeutic Efficacy of Oncolytic Herpes Simplex Virus-1 with Integrin β1 Blocking Antibody OS2966

Tae Jin Lee[1], **Mitra Nair**[1], **Yeshavanth Banasavadi-Siddegowda**[1,2], **Joseph Liu**[3], **Tejaswini Nallanagulagari**[3,4], **Alena Cristina Jaime-Ramirez**[3], **Jeffrey Yunhua Guo**[3,5], **Haroon Quadri**[6], **Jianying Zhang**[7], **Kurt H Bockhorst**[8], **Manish K Aghi**[9], **W. Shawn Carbonell**[10], **Balveen Kaur**[1], and **Ji Young Yoo**[1]

[1]The Department of Neurosurgery, University of Texas Health Science Center at Houston, Houston, TX, 77030;

[2]Surgical Neurology Branch, NINDS, National Institutes of Health, Bethesda, MD;

[3]Department of Neurological Surgery;

[4]Biochemistry and Microbiology Majors,

[5]Biology Major, James Comprehensive Cancer Center, The Ohio State University Wexner Medical Center, Columbus, OH, 43210;

[6]Northeast Ohio Medical University, Rootstown, OH, 44272;

[7]Center for Biostatistics, Department of Biomedical Informatics, James Comprehensive Cancer Center, The Ohio State University Wexner Medical Center, Columbus, OH, 43210;

[8]Department of Diagnostic and Interventional Imaging, University of Texas Health Science Center at Houston, Houston, TX, 77030;

[9]University of California at San Francisco;

[10]OncoSynergy, Inc., South San Francisco, CA, 94080

Abstract

Integrin β1 receptor, expressed on the surface of tumor cells and macrophages in the tumor microenvironment (TME), has been implicated in both tumor progression as well as resistance to multiple modalities of therapy. OS2966 is the first clinical-ready humanized monoclonal antibody to block integrin β1 and was recently orphan designated by FDA Office of Orphan Products Development (OOPD). Here, we tested therapeutic potential of OS2966-mediated integrin β1 blockade to enhance the efficacy of oncolytic herpes simplex virus-1 (oHSV) through evaluation of virus replication, tumor cell killing efficiency, effect on the antiviral signaling pathway, co-culture assays of oHSV-infected cells with macrophages, and *in vivo* bioluminescence imaging on mammary fat pad triple negative breast cancer xenograft and subcutaneous and intracranial glioma

Corresponding author information: Ji Young Yoo PhD, Department of Neurosurgery, University of Texas Health Science Center at Houston, 6431 Fannin St. MSE R117A, Houston, TX, 77030, Ji.Young.Yoo@uth.tmc.edu, Tel: 713-500-6173.

Disclosure of Potential Conflicts of Interest

WSC is a co-founder, employee, Director and shareholder of Oncosynergy, Inc. WSC and MKA are inventors of patents related to OS2966.

Author Manuscript Author Manuscript Author Manuscript Author Manuscript

xenografts. OS2966 treatment decreased interferon signaling and pro-inflammatory cytokine induction in oHSV-treated tumor cells and inhibited migration of macrophages, resulting in enhanced oHSV replication and cytotoxicity. OS2966 treatment also significantly enhanced oHSV replication and oHSV-mediated anti-tumor efficacy in orthotopic xenograft models including triple negative breast cancer and glioblastoma. The results demonstrated the synergistic potential of the combinatory treatment approach with OS2966 to improve anti-tumor efficacy of conventional oHSV therapy.

Introduction

Oncolytic viruses (OVs) are either genetically engineered or carefully chosen strains to retain their natural propensity of replication in neoplastic cells. Thus, the infection of tumor cells with OVs can result in tumor destruction with minimal toxicity to adjacent non-neoplastic tissues. OV therapy has been recently approved by FDA for the treatment of metastatic melanoma (1). Many second-generation oncolytic herpes simplex virus (oHSV) vectors have been generated and are currently being tested at different stages in clinical trials for breast cancer (NCT02779855 and NCT03004183) and GBM (NCT00028158, NCT02062827, and NCT00157703).

Tumor microenvironment (TME) plays a critical role during cancer progression and in determining response to therapeutics. oHSV therapy-induced changes in the TME can have consequences that both augment therapeutic outcome and also confer resistance (2). Treatment of tumors with OVs can also cause a surge in the immune response, which can have the potential to activate anti-tumor immunity. However, the inflammatory environment can also promote the regrowth of residual cancer cells after virus clearance. Thus, a better understanding of microenvironmental changes induced by OV treatment in the TME is essential to improve the therapeutic efficacy of OVs.

Integrin β1 is the dominant subunit represented in all four classes of integrin receptors involved in multiple functions such as cellular proliferation, invasion and inflammation (3). Integrin α6 is highly expressed in the both breast and glioma stem cells (4) and $\alpha_6\beta_1$ has been shown to regulate neural stem cell division (5). Inhibition of integrin β1 has shown anti-tumor efficacy in preclinical models of brain and breast cancer cells (6–9) through modulation of multiple cancer hallmarks (10, 11). Integrin β1 has also been shown to play a critical role in phagocytosis of microbial pathogens and phagosome maturation in macrophages (12).

OS2966 is a humanized integrin β1 (CD29) blocking antibody and has shown significant anti-tumor efficacy in several preclinical models including metastatic ovarian, triple negative breast and therapy-resistant glioblastoma (6, 13). Recently, OS2966 has been granted orphan designation by the FDA Office of Orphan Products Development (OOPD) in the treatment of glioblastoma and ovarian cancer. In this study, we hypothesized that blockade of integrin β1 by OS2966 may enhance the therapeutic index of oHSV therapy against solid tumors.

Author Manuscript Author Manuscript Author Manuscript Author Manuscript

Materials and methods

Cell lines and Oncolytic Herpes Simples Virus-1 (oHSV-1)

U251T3, U87ΔEGFR, and LN229 (glioblastoma cell lines); MDA-231 and MDA-468 (triple-negative breast cancer cell lines); and Vero cells were maintained in Dulbecco's modified eagle's medium (DMEM; Gibco BRL, Grand Island, NY) supplemented with 10% fetal bovine serum (FBS). LN229 and U251 cells were obtained from Dr. Erwin G. Van Meir (Emory University, Atlanta, GA), and U251-T3 cell was created in our laboratory as a tumorigenic clone of U251 cells by serially passaging these cells three times in mice. U87ΔEGFR cell expressing a constitutively active truncated mutant form of epidermal growth factor receptors (EGFRvIII) was obtained from Dr. Frank Furnari (University of San Diego) (14). Monkey kidney epithelial derived Vero cell was purchased from ATCC. MDA-231 and MDA-468 (human breast cancer) cells were obtained from Dr. Michael C. Ostrowski (Ohio State University, Columbus, OH) (15). All human cell lines were authenticated by the STRS profiling, and maintained in culture for less than 50 passages after authentication. GBM30, GBM12 and GBM34 patient-derived primary GBM cells were maintained as tumor spheres in DMEM/F12 medium supplemented with 2% B27, human EGF (20 ng/ml) and bFGF (20 ng/ml) in low-attachment cell culture flasks. These cells were authenticated by the University of Arizona Genetics Core via STR profiling in July 2013, and maintained for no more than 50 passages after authentication. Murine RAW264.7 macrophages obtained in June 2010 from Dr. S. Tridandapani (Ohio State University, Columbus, OH) were maintained in RPMI supplemented with 5% FBS. All cells were maintained at 37°C in a humidified atmosphere with 5% carbon dioxide and maintained with 100 units of penicillin/mL, and 0.1 mg of streptomycin/mL (Penn/Strep). All cells were routinely monitored for the changes in morphology and growth rate. All cells were confirmed as negative for *Mycoplasma*. rHSVQ1 and rHSVQ1-IE4/5-Luciferase (rHSVQ1-Luc) carry disrupted UL39 locus with homozygous deletion of γ34.5 gene. rHSVQ1-Luc contains the luciferase transgene under the HSV-1 IE4/5 promoter (16).Viral stocks were generated and tittered on Vero African green monkey kidney cells (American Type Culture Collection, Manassas, VA) via a standard plaque forming unit assays, as previously described (17, 18).

Integrin β1 blocking antibody OS2966

OS2966 is a patented humanized monoclonal IgG1 against CD29/beta1 integrin (U.S. patent No. 10023638 B2, Inventor: W. Shawn Carbonell, 2018) (https://patentimages.storage.googleapis.com/1d/6b/1a/10640237ac67d5/US10023638.pdf). It has been under development by OncoSynergy, Inc. for clinical therapeutic purpose for oncology and other indications. OS2966 uses humanized variant H3 (variant region ID: VH4VK4; correnspnding VH and VK sequence ID No. 12 and 22 respectively as described in the Table 2 in the Patent No. 10023638 B2). OS2966 used in this study was provided by OncoSynergy, Inc as research grade produced by a contract manufacturer in a 100L pilot scale bioreactor, purified, and formulated in sterile PBS at the concentration of 5.87 mg/ml (6, 7, 13).

Author Manuscript Author Manuscript Author Manuscript Author Manuscript

Cell Migration Assay

Cell migration was evaluated in a 24-well chemotaxis chamber equipped with a polycarbonate filter with 5 μm pores (Costar, Corning, NY). LN229 cells were plated in the bottom chamber followed by virus infection for 1 hour at multiplicity of infection (MOI) of 1. After unbound viruses were washed out, the cells were treated with 10 μg/ml of IgG or OS2966 for 4 hours. Subsequently, serum starved Raw264.7 cells were plated in the top chamber to migrate for 6 hours. Cells that traversed the membrane were fixed and stained with crystal violet, while non-migrated cells were removed with a cotton-tipped applicator. Cells from at least three different transwells were quantified by averaging counts from three random views at ×20 magnification.

Real-time PCR

Cells were harvested by centrifugation for 5 minutes at 8,000 rpm and homogenized using a QIAshredder (Qiagen, Valencia, CA). Total RNAs were isolated using RNeasy Mini Kit (Qiagen, Valencia, CA) and subjected to quantitative real Time PCR (qRT-PCR) using SyBr Green qPCR Master Mix (Applied Biosystems, Carlsbad, CA). GAPDH was used as an internal control with relative quantification being expressed as a ratio of the difference in the number of cycles needed for expression of a gene. Detection primers were designed using the Primer Express Program (Applied Biosystems, Carlsbad, CA) (Supplementary Table S1).

In vitro *viral replication assay*

Cells were plated in 6-well plates with 2F DMEM and infected with viruses at MOI of 0.002 for one hour. After the removal of unbound viruses, the cells were treated with 10 μg/ml of human IgG or OS2966. Seventy-two hours after the virus infection, both cells and media were collected and subjected to repeated freezing and thawing for three times to release the viruses. The number of infectious particles present in the resulting supernatant was determined by performing a standard plaque forming unit assay on Vero cells. All assays were performed in triplicate.

Western blot analysis and antibodies

Cell lysates were fractionated by SDS-PAGE and transferred to a polyvinylidene difluoride (PVDF) membrane. After blocking, the membrane was incubated with primary antibodies against CCN1 (Santa Cruz Biotechnology, Santa Cruz, CA); phospho-Stat1 and total Stat1 (BD Transduction Laboratories, San Diego, CA); β-tubulin (Cell Signaling Technology, Waltham, MA); phospho-FAK (S359), total FAK, ITGB1 and GAPDH (Abcam, Cambridge, MA) (each diluted 1:1000) followed by either HRP-conjugated secondary anti-mouse antibody (each diluted 1:1000) (GE Healthcare, Piscataway, NJ) or HRP-conjugated secondary goat anti-rabbit antibody (each diluted 1:1000) (Dako, Hamburg, Germany). Immunoreactive bands were visualized using enhanced chemiluminescence (ECL) (GE Healthcare, Piscataway, NJ).

Author Manuscript Author Manuscript Author Manuscript Author Manuscript

Xenograft studies

All mouse housing and experiments were performed in accordance with the Subcommittee on Research Animal Care of the Ohio State University (OSU) guidelines and have been approved by the Institutional Review Board. Four-week-old outbred female athymic nu/nu mice were obtained from the Target Validation Shared Resource at the Ohio State University, from which original breeders (strain #553 and #554) were received from the NCI Frederick facility.

For subcutaneous tumor studies, 1×10^7 U87ΔEGFR human glioma cells were implanted into the rear flank of nude mice. When tumors reached an average size of 150 mm^3, the tumor-implanted mice were randomly grouped and intraperitoneally treated with IgG or OS2966 (5 mg/kg) twice a week. At day 2 from the OS2966 treatment, PBS or rHSVQ-Luc were administered intratumorally (1×10^5 PFU).

For orthotopic breast carcinoma studies, 1×10^7 of MDA468 human breast cancer cells were injected into the mammary fat pad of nude mice. When the tumor reached an average size of 150 mm^3, tumor-implanted mice were randomly grouped and intraperitoneally treated with control IgG or OS2966 (5 mg/kg) for 1 day prior to oHSV treatment and twice a week thereafter during the duration of the study. At day 2 and day 6 from the OS2966 treatment, PBS or rHSVQ-Luc were then administered intratumorally (1×10^5 PFU). Tumor volume was calculated based on tumor length and width using the following formula: volume = $0.5LW^2$.

For intracranial glioma xenograft studies, anesthetized nude mice were fixed in a stereotactic apparatus, and a burr hole was drilled at 2 mm lateral and 1 mm front to the bregma to a depth of 3.5 mm. Patient derived primary GBM cells (GBM12) were implanted through the burr hole in 2 μl Hank's buffered salt solution. Eight days post tumor cell implantation, mice were randomly grouped and injected with control IgG, OS2966, oHSV, or combination of oHSV with OS2966. Two days prior to the oHSV treatment, mice were injected intratumorally with control IgG or OS2966 (5 mg/kg) and twice a week thereafter for one month. At day 10 from the tumor implantation, mice were injected intratumorally with PBS or 1×10^5 pfu of rHSVQ1-Luc through the same burr hole. Animals were monitored daily and subjected to euthanization when they showed sign of morbidity (hunched posture and weight loss).

In vivo luciferase imaging

Nude mice established with subcutaneous U87ΔEGFR or orthotopic MDA468 tumors were treated with control IgG or OS2966 (5 mg/kg) by intraperitoneal injection at days −2, 0, 2, and 4. Two days post control IgG or OS2966 treatment, the mice were treated with rHSVQ1-Luc of 1×10^5 pfu by intratumoral injection and subjected to *in vivo* luciferase imaging at days 1, 2, 3, 4, and 5 after the oHSV injection. Briefly, mice were injected with Luciferin substrate solution (25 mg/ml in PBS, dose of 100 mg/kg, Perkin Elmer, Waltham, MA) by an intraperitoneal injection followed by anesthesia. The anesthetized mice were placed on non-fluorescent black paper on the imaging platform under ZFOV-24 zoom lens-installed IVIS Lumina Series III Pre-clinical In Vivo Imaging System (Perkin Elmer,

Author Manuscript Author Manuscript Author Manuscript Author Manuscript

Waltham, MA) to reduce background noise. Luminescence intensity was expressed as Averaged Radiance [p/s/cm^2/sr], then normalized by tumor volume (mm^3) obtained by MRI.

Statistical analysis

To compare two independent treatments for continuous endpoints such as viral titers, and cell viability assay, Student's t-test was used. When multiple pairwise comparisons were made, one-way ANOVA was used. To evaluate the synergistic interaction between OS2966 and oHSV, an interaction contrast or two-way ANOVA model was applied. Synergistic effect represents that the combined treatment produced an effect (versus control) greater than the additive effect of two single treatments (versus control, respectively). Log-rank test was used to compare survival curves for survival data and cox regression model was used to evaluate the synergistic interaction between OS2966 and oHSV on survival data. *p* values were adjusted for multiple comparisons by Holms' procedure. A *p* value of 0.05 or less was considered statistically significant.

Results

OS2966 treatment increases oHSV replication and tumor cell killing

Integrin β1 binds to an integrin-downstream effector kinase, focal adhesion kinase (FAK), which activates both Stat1 and Akt. The FAK-mediated activation of Stat1 and Akt involves integrin-mediated cell adhesion and migration, and enhances oncogenic transformation (22, 23). Validation of OS2966 as an inhibitor of downstream signaling from integrin β1 was confirmed by Western-blot analysis on tumor cells treated with oHSV in the presence or absence of OS2966. Reduced phosphorylation levels of FAK and AKT indicated the functionality of OS2966 as a function-blocking antibody of integrin signaling pathway. Furthermore, increased cleaved PARP was observed in the oHSV-infected cells in the presence of OS2966, indicating an increased tumor cell killing by oHSV (Fig. 1A). To evaluate the impact of integrin β1 blockade by OS2966 on the therapeutic efficacy of oHSV, patient derived primary GBM neurosphere cells were grown onto laminin (LM, ligands for integrin receptors $\alpha_2\beta_1$ and $\alpha_6\beta_1$)- and fibronectin (FN, ligand for integrin receptors $\alpha_v\beta_1$, $\alpha_3\beta_1$, $\alpha_4\beta_1$, $\alpha_5\beta_1$, and $\alpha_8\beta_1$)-coated plates and treated with oHSV in the presence or absence of OS2966. Consistent with the role of integrin β1 in adhesion to ECM, OS2966 treated cells showed reduced cell adhesion, indicating dissociation from ECM (Fig. 1B bright field: compare panels a to b and c to d). Since oHSV encodes GFP, oHSV infected cells were visualized as GFP positive under fluorescence microscopy. Fluorescence microscopy revealed an apparent increase in the population of GFP-positive cells with OS2966 treatment, which indicates an increased viral replication (Fig. 1B). The increased virus replication was also confirmed by quantification of viral titers. Both breast cancer and glioma cell lines, as well as patient derived primary GBM cells, showed a significant increase in viral titers with OS2966 treatment (Fig. 1C). Consistent with the increased viral replication (Fig. 1B–C) and increased level of cleaved PARP (Fig. 1A), significantly reduced cell viability was observed in the cells treated with both OS2966 and oHSV compared to either OS2966 or oHSV alone treated cells (Fig. 1D). Collectively, these data indicate that the combination treatment of oHSV with OS2966 enhances tumor cell killing efficiency through increased viral replication.

Author Manuscript Author Manuscript Author Manuscript Author Manuscript

OS2966 treatment inhibits oHSV-induced type-I IFN signaling

It has been previously shown that oHSV infection triggers an activation of signal transducers and activators of transcription 1 (Stat1), which activates an innate antiviral defense response mechanism resulting in virus clearance from the oHSV infected cells (21). We have also observed that the activation of integrin β1 contributes to Stat1 activation and constrains oHSV therapeutic efficacy (19). To evaluate the effect of OS2966 on the oHSV-induced type-I IFN response, we evaluated gene expression changes in the type-I IFN pathway in the tumor cells treated with or without oHSV in the presence of OS2966. Consistent with previous reports, the induction of Stat1, IFNα and IFNβ was clearly observed after oHSV-treatment. Interestingly, co-treatment of oHSV with OS2966 significantly attenuated the oHSV-mediated induction of type-I IFN response genes (Fig. 2A). In addition, the expression level of downstream anti-viral IFN responsive genes, such as OAS1, OAS2, IRF3, IRF9 and PKR was significantly reduced in the oHSV-infected cells treated with OS2966 (Fig. 2B). Western blotting analysis also showed the suppression of oHSV-induced phosphorylation of Stat1 by the presence of OS2966, further confirming the impact of OS2966 on type-I IFN defense signaling (Fig. 2C). Previously, we have also shown that oHSV infection leads to the induction of CCN1 in the extracellular tumor microenvironment (TME) and that CCN1 can bind and activate integrin β1 (19). In the current study, oHSV-mediated induction of CCN1 expression at both gene and protein levels was also attenuated by OS2966 treatment (Fig. 2B–C). This underscores the significance of integrin β1 in CCN1 induction upon HSV infection.

OS2966 treatment inhibits oHSV-induced macrophage activation and migration

Our previous study showed that CCN1 contributes towards MCP-1 mediated crosstalk between oHSV-infected tumor cells and macrophages (20). To evaluate the impact of OS2966 on oHSV infection-induced MCP-1 production from the infected tumor cells, an expression change of MCP-1 was measured in the indicated cancer cells. A robust induction of MCP-1 gene expression was observed in both breast cancer and glioma cells after oHSV treatment, however OS2966 co-treatment significantly reduced the oHSV infection-mediated MCP-1 induction (Fig 3A) To further evaluate the consequence of reduced MCP-1 gene expression by OS2966 treatment, we measured macrophage cell migration towards oHSV-infected glioma cells (20). Briefly, OS2966 or control IgG was added to oHSV-infected tumor cells in the bottom chamber of a transwell plate and migration level of serum starved macrophage cells placed in the top chamber was measured (Fig. 3B). OS2966 co-treatment significantly suppressed macrophage cell migration towards oHSV-infected tumor cells compared to control IgG (Fig. 3C–D). Interestingly, OS2966 treatment to non-oHSV infected cancer cells also reduced macrophage chemotaxis suggesting a MCP-1 independent reduction mechanism. To further unveil a functional mechanism of the OS2966-mediated inhibition of oHSV-induced interferon signaling and macrophage migration, an *in vitro* co-culture system was employed as previously described (21). Briefly, mCherry-expressing primary GBM cells (GBM30-mCherry) were sequentially treated with oHSV and either OS2966 or control IgG and overlaid with serum starved Raw264.7 murine macrophage cells. Visualization of GFP-positive cells overlapped with mCherry signals indicate virus replications in the oHSV-infected glioma cells. As expected from the reduction of interferon signaling and macrophage migration by OS2966, both visualization of GFP-positive infected

Author Manuscript Author Manuscript Author Manuscript Author Manuscript

cells and quantification of virus replication in glioma cells cultured in proximity to macrophages revealed that OS2966 treatment enhanced oHSV replication even in the presence of macrophages (Fig. 3E–F). These observations strongly indicated that co-treatment of OS2966 with oHSV can benefit viral replication by inhibiting oHSV-induced macrophage activation.

OS2966 treatment enhances oHSV replication and anti-tumor efficacy in vivo

As observed above, the combination treatment of oHSV with OS2966 significantly inhibited anti-viral response in the oHSV-infected cancer cells and enhanced virus replication and tumor cell killing *in vitro*. To test the translational relevance, we examined the impact of OS2966 treatment on virotherapy *in vivo* by using firefly luciferase expressing oHSV, rHSVQ1-IE4/5-Luciferase (oHSV-Luc), in orthotopic breast cancer-bearing mice. Briefly, mice implanted with MDA468 tumor in their mammary fat pad were pre-treated with OS2966 or control IgG by intraperitoneal injection one-day prior to the intra-tumoral injection of oHSV-Luc. Virus propagation was demonstrated by *in vivo* bioluminescence imaging of the mice for luciferase activity as a surrogate metric. The mice treated with OS2966 showed a significant increase of virus-expressing luciferase signals compared to the mice treated with control IgG, indicating an increased virus replication in the tumor region (oHSV+IgG vs oHSV+OS2966 total flux: 89636.5 ± 63455.89 vs 311398.3 ± 234748.9, $p = 0.0495$) (Fig. 4A–B). In addition to the enhanced virus replication, the combination treatment of OS2966 with oHSV significantly enhanced anti-tumor efficacy as demonstrated by a 100% response rate (Fig. 4C). Indeed, mean tumor volumes in the mice treated with the combination of OS2966 with oHSV were dramatically diminished to 29.6 mm^3 by day 21 compared to 322.16 mm^3 in the mice co-treated with oHSV-Luc and control IgG (oHSV-Luc + IgG vs oHSV-Luc + OS2966 respectively, $p < 0.001$) (Fig. 4C). These data correlated to 10.9-fold reduction in tumor growth compared to control IgG and oHSV-Luc-treated mice. After 21 days of the treatment with the oHSV and OS2966, 3 out of 6 mice (50%) showed completely regressed tumors. Furthermore, significantly increased necrosis was observed in 100% of tumors treated with both oHSV and OS2966, indicating enhanced virus replication (Supplementary Fig. S1). A similar increase of virus replication and tumor growth suppression was also observed in mice bearing subcutaneous U87ΔEGFR glioblastoma xenograft tumors (Fig. 4D–F). As observed in the mammary fat pad mice models, the mice showed increased levels of virus-expressing luciferase compared to the mice treated with control IgG (oHSV+IgG vs oHSV+OS2966 total flux: 2303.633 ± 1374.113 vs 97146.67 ± 18839.17, $p < 0.001$) (Fig. 4D–E). Evidently, the increased virus replication also significantly reduced tumor growth (Fig 4F). Systemic delivery of OS2966 by intraperitoneal injection did not enhance virus replication in mice bearing intracranial tumors (both U87ΔEGFR and patient derived primary GBM (GBM30)) (Supplementary Fig. S2). Consistent with no difference in virus replication between IgG+oHSV and OS2966+oHSV, combination treatment with OS2966 and oHSV also did not enhance mice survival rate in intracranial GBM30-bearing mice (Supplementary Fig. S3). These results may be explained by insufficient delivery of OS2966 to tumor cells in this model, particularly with regards to the orthotopic study where the large IgG molecule is not likely to penetrate the intact blood brain barrier (BBB). Thus, we tested whether OS2966 treatment by intratumoral (IT) injection can enhance oHSV therapeutic efficacy in the intracranial

Author Manuscript Author Manuscript Author Manuscript Author Manuscript

xenograft model (Fig. 5). Briefly, intracranial patient derived primary GBM (GBM12)-bearing mice were treated with 5 mg/kg of OS2966 or control IgG by IT injection beginning 9 days post tumor implantation followed by IT injection of oHSV-Luc of 1×10^5 pfu at the next day. Thereafter, the mice were treated with IgG or OS2966 twice a week for 1 month by IT injection. *In vivo* tumor growth was measured by contrast-enhanced magnetic resonance imaging (MRI) to non-invasively measure the tumor volume. MRI analysis revealed that the combination treatment with OS2966 and oHSV significantly reduced tumor size compared to the oHSV+IgG treatment (Fig. 5A–B). More importantly, the combination treatment with oHSV and OS2966 significantly improved the survival rate of the mice compared to the mice treated with either oHSV or OS2966 alone (Fig. 5C). Taken together, these data strongly demonstrate that systemic or IT administration of OS2966 can significantly enhance oHSV replication *in vitro* and *in vivo* leading to enhanced therapeutic efficacy of oHSV *in vivo* (Fig. 5), suggesting immediate translational potential in human clinical trials.

Discussion

Oncolytic herpes simplex virus-1 (oHSV) derived virotherapy offers new therapeutic potential to improve the patient survival and the quality of life through tumor cell-specific replication and lysis with concurrent activation of adaptive anti-tumor immune responses. Multiple oHSV vectors have been generated and some of them are currently being evaluated at different stages in clinical trials. Talimogene Laherparepvec (T-VEC, Imlygic®), a HSV type 1-derived oncolytic immunotherapy, has been recently approved by FDA for the treatment of advanced metastatic melanoma. As the safety and efficacy of T-VEC is being actively evaluated for the treatment of many different cancer types, it may become an attractive alternative treatment option for chemotherapy-resistant cancers (1). Tumor microenvironment (TME) has been increasingly recognized as a key player determining the growth and progression of tumors and also their response to therapy. A better understanding on the impact of virotherapy on tumor and TME can help to develop a clinically promising strategy to enhance anti-tumor efficacy of oHSV. Here, we evaluated therapeutic efficacy of an IND-ready integrin β1 neutralizing antibody, OS2966, in conjunction with oHSV therapy.

Integrins are transmembrane cell surface receptors compromised of 18 α- and 8 β- subunits, which pair to produce a total of 24 different functional integrins (22). The integrin dimers bind with multitude extracellular matrix (ECM) molecules including fibronectin (FN) and laminin (LM) and play an important role in sensing the TME and regulating the cell survival proliferation, invasion, and cancer therapeutic resistance of malignant tumors (23). We have previously identified cysteine-rich angiogenic inducer 61 (CCN1) as an extracellular matrix (ECM) protein that is actively secreted by oHSV-infected tumor cells. In tumor ECM, CCN1 binds to integrins on the surface of tumor cells ($\alpha_6\beta_1$) and macrophages ($\alpha_M\beta_2$) and triggers antiviral type-I interferon and chemokine responses that increase macrophage infiltration and activation. These interactions cause increased virus clearance in solid tumors, thereby limiting oncolytic virus therapeutic efficacy (19, 20, 24, 25). The binding of FN to integrins in the macrophage cells activates the integrin-downstream effector kinase, focal adhesion kinase (FAK) signaling, activating macrophage cell migration (26). Integrin β1 plays critical role as a key signaling receptor in regulating phagosome maturation and microorganism clearance in macrophages (27). In this study, we showed that the inhibition of integrin β1

Author Manuscript Author Manuscript Author Manuscript Author Manuscript

signaling with OS2966 significantly suppresses oHSV therapy-induced the activation of antiviral type-I interferon signaling (Fig. 2) and improves virus replication *in vitro* (Fig. 1 and 3) and *in vivo* (Fig. 4), resulting in improved therapeutic efficacy (Fig. 5). Our findings are bolstered by recent studies showing that blockade of FAK/AKT pathway is linked to suppression of anti-viral interferon stimulated gene expression (28–30).

In tumor cells, integrin β1 is known to recruit FAK and induce its autophosphorylation and downstream Akt phosphorylation promoting tumor cell growth (31). The binding of ECM proteins such as CCN1 and LM to integrins activates FAK signaling, which can promote tumor progression and metastasis through effects on cancer cells as well as stromal cells of the TME. Our results indicated that the OS2966 treatment significantly reduced the phosphorylation of FAK and Akt in the presence and absence of oHSV (Fig. 1A). Consistent with previous reports demonstrating that wild-type HSV induces rapid phosphorylation of FAK as important for HSV entry by promoting transport/delivery of viral capsids to the nuclear pore (32), we observed significantly increased phosphorylation of FAK and Akt in the oHSV treated tumor cell (Fig. 1A). However, the inhibition of integrin β1 signaling with OS2966 significantly suppressed oHSV infection-induced activation of FAK-Akt signaling pathway and thereby increased PARP cleavage, indicating enhanced tumor cell killing by the combination treatment with OS2966 and oHSV (Fig. 1A). More importantly, although FAK activation is known to be required for wild type HSV-1 virus entry and knock down of FAK is shown to reduce the translocation of wild type HSV capsid into the nucleus (33), the OS2966 treatment did not suppress oHSV replication efficacy in cancer cells (Fig. 1B–C). The inhibition of FAK phosphorylation observed via blockade of upstream integrin ß1 receptor (with OS2966) has likely distinct biological implications compared to FAK knock down described in the previous report (32). The different results obtained from integrin β1 blockade and FAK knock down might also be due to the fact that while we have focused on attenuated oncolytic HSV-1 (F strain viruses) that are clinically relevant for therapy, the prior report has used exclusively wild type HSV (KOS strain virus) in a human cervical epithelial cell line (CaSki). Collectively, despite the suppression of oHSV-induced FAK phosphorylation, our data indicated that the OS2966 treatment-induced IFN signaling inhibition strongly improved oHSV replication *in vitro* and *in vivo*.

Insulin-like growth factor-binding protein 2 (IGFBP2) is overexpressed in breast cancer and GBM and activates integrin β1, resulting in downstream tumor cell proliferation and invasion pathways (34). Integrin β1 expression is also correlated with bevacizumab resistance in GBM patients (6) and integrin α6β1 contributes to the survival of breast carcinoma cells under stress conditions through upregulation of VEGF expression, either at the level of transcription or translation (35). Integrin β1-containing filopodium-like protrusions activate tumor cells and promotes tumor cell proliferation and metastasis (36, 37). Apart from direct tumor cell and ECM interactions, integrins are also known to engage in crosstalk with growth factor receptors, such as EGFR, in the cell cycle progression in cancer cells. Several studies have implicated that integrin β1 functions during origination, growth, progression and therapeutic resistance of solid tumors, including GBM and breast cancer with brain metastasis, by promoting stromal and growth factor derived oncogenic signaling (38, 39). More recently, downregulation of integrin β1 inhibited mesenchymal function in resistant GBM cells and decreased phosphorylations of EGFR and c-Met in

Author Manuscript Author Manuscript Author Manuscript Author Manuscript

hepatocytes during liver regeneration (6, 7, 40). A novel transactivating complex of c-Met and integrin β1 has been described to drive metastasis and invasive resistance in metastatic breast cancer and therapy-resistant glioblastoma (41). OS2966, an IND-ready integrin β1 neutralizing antibody, was shown to disrupt this unique receptor complex which may be an additional feature of its many mechanisms of action (6, 13).

In both orthotopic breast and subcutaneously implanted glioma xenograft models, we observed enhanced anti-tumor efficacy when we treated OS2966 systemically by intraperitoneal injection as monotherapy and in combination with IT oHSV. However, systemic delivery of OS2966 did not result in replication enhancement of IT administered oHSV in two orthotopic glioblastoma models. This can be explained by the BBB which particularly excludes macromolecules such as OS2966, a full-length IgG1, from entering the central nervous system (CNS). Even in the case where CNS entry may occur in tumor areas with BBB breakdown, diffusion in the brain is highly limited, resulting in inadequate drug distribution. In contrast, and consistent with this hypothesis, when we directly delivered OS2966 and oHSV intralesionally via IT injection to orthotopic glioblastoma xenografts we demonstrated a highly significant survival advantage with the combination therapy. Although the local delivery of biologics into the CNS of preclinical model systems is inherently difficult, in the clinic, delivering both drugs and biologics directly to the site of disease in the CNS is possible with specialized catheter systems which are being actively investigated in multiple centers worldwide. These convection enhanced delivery (CED) methods include precise 3-D neuronavigation for lesion targeting, bespoke FDA-cleared CED catheters specifically designed to minimize reflux, and positive real-time confirmation of payload delivery through intraoperative MR imaging (42, 43). Additional advantages of local, rather than systemic, delivery of both OS2966 and oHSV in the clinical setting include 1) prevention of unnecessary systemic exposure in patients, 2) a possible decrease in costs by minimizing the amount of material per dose by orders of magnitude and 3) assurance of more consistent targeted delivery at the appropriate therapeutic level throughout the area of distribution. Therefore, these results have immediate translational potential.

Here, we show for the first time to our knowledge that oHSV therapeutic efficacy can be enhanced through concurrent treatment with an integrin β1 neutralizing antibody, OS2966. The current study was to assess the hypothesis that combining oHSV with OS2966 may improve the therapeutic index of this approach by releasing the brakes on oHSV replication. In this study, we demonstrated that the OS2966 treatment significantly inhibited innate antiviral defense responses as well as tumor cell proliferation. Additionally, oHSV treatment significantly enhanced integrin β1 expression in a dose dependent manner (Supplementary Fig. S4), suggesting that oHSV treatment may also sensitize tumors to OS2966 treatment. Furthermore, inhibition of integrin β1 signaling by OS2966 treatment reduced the induction of integrin β1activating ECM proteins like CCN1. These findings may accelerate the successful translation of oHSV-based combination therapies into durable outcomes for cancer patients.

Supplementary Material

Refer to Web version on PubMed Central for supplementary material.

Author Manuscript Author Manuscript Author Manuscript Author Manuscript

Acknowledgments

This study was supported in part by: ACS grant IRG-67-003-50 to J.Y. Yoo; NIH grant P30 DK056338 to T.J. Lee; NIH grants R01 NS064607, R01 CA150153, and P01CA16320 to B. Kaur. We would like to acknowledge Dr. Joanna O'Leary for critical reading of the manuscript.

References

1. Andtbacka RH, Kaufman HL, Collichio F, Amatruda T, Senzer N, Chesney J, et al. Talimogene Laherparepvec Improves Durable Response Rate in Patients With Advanced Melanoma. J Clin Oncol. 2015;33(25):2780–8. [PubMed: 26014293]
2. Kaur B, Chiocca EA, Cripe TP. Oncolytic HSV-1 virotherapy: clinical experience and opportunities for progress. Curr Pharm Biotechnol. 2012;13(9):1842–51. [PubMed: 21740359]
3. Huck L, Pontier SM, Zuo DM, Muller WJ. beta1-integrin is dispensable for the induction of ErbB2 mammary tumors but plays a critical role in the metastatic phase of tumor progression. Proc Natl Acad Sci U S A. 2010;107(35):15559–64. [PubMed: 20713705]
4. Lathia JD, Gallagher J, Heddleston JM, Wang J, Eyler CE, Macswords J, et al. Integrin alpha 6 regulates glioblastoma stem cells. Cell Stem Cell. 2010;6(5):421–32. [PubMed: 20452317]
5. Loulier K, Lathia JD, Marthiens V, Relucio J, Mughal MR, Tang SC, et al. beta1 integrin maintains integrity of the embryonic neocortical stem cell niche. PLoS Biol. 2009;7(8):e1000176. [PubMed: 19688041]
6. Carbonell WS, DeLay M, Jahangiri A, Park CC, Aghi MK. beta1 integrin targeting potentiates antiangiogenic therapy and inhibits the growth of bevacizumab-resistant glioblastoma. Cancer Res. 2013;73(10):3145–54. [PubMed: 23644530]
7. Jahangiri A, Aghi MK, Carbonell WS. beta1 integrin: Critical path to antiangiogenic therapy resistance and beyond. Cancer Res. 2014;74(1):3–7. [PubMed: 24327727]
8. Park CC, Zhang H, Pallavicini M, Gray JW, Baehner F, Park CJ, et al. Beta1 integrin inhibitory antibody induces apoptosis of breast cancer cells, inhibits growth, and distinguishes malignant from normal phenotype in three dimensional cultures and in vivo. Cancer Res. 2006;66(3):1526–35. [PubMed: 16452209]
9. Huang C, Park CC, Hilsenbeck SG, Ward R, Rimawi MF, Wang YC, et al. beta 1 integrin mediates an alternative survival pathway in breast cancer cells resistant to lapatinib. Breast Cancer Res. 2011;13(4).
10. Blandin AF, Renner G, Lehmann M, Lelong-Rebel I, Martin S, Dontenwill M. beta1 Integrins as Therapeutic Targets to Disrupt Hallmarks of Cancer. Front Pharmacol. 2015;6:279. [PubMed: 26635609]
11. Pickup MW, Mouw JK, Weaver VM. The extracellular matrix modulates the hallmarks of cancer. EMBO Rep. 2014;15(12):1243–53. [PubMed: 25381661]
12. Wang QQ, Li H, Oliver T, Glogauer M, Guo J, He YW. Integrin beta 1 regulates phagosome maturation in macrophages through Rac expression. J Immunol. 2008;180(4):2419–28. [PubMed: 18250451]
13. Campbell MR, Zhang H, Ziaee S, Ruiz-Saenz A, Gulizia N, Oeffinger J, et al. Effective treatment of HER2-amplified breast cancer by targeting HER3 and beta1 integrin. Breast Cancer Res Treat. 2016;155(3):431–40. [PubMed: 26860947]
14. Narita Y, Nagane M, Mishima K, Huang HJS, Furnari FB, Cavenee WK. Mutant epidermal growth factor receptor signaling down-regulates p27 through activation of the phosphatidylinositol 3-kinase/Akt pathway in glioblastomas. Cancer Res. 2002;62(22):6764–9. [PubMed: 12438278]
15. Meisen WH, Dubin S, Sizemore ST, Mathsyaraja H, Thies K, Lehman NL, et al. Changes in BAI1 and nestin expression are prognostic indicators for survival and metastases in breast cancer and provide opportunities for dual targeted therapies. Mol Cancer Ther. 2015;14(1):307–14. [PubMed: 25376607]
16. Terada K, Wakimoto H, Tyminski E, Chiocca EA, Saeki Y. Development of a rapid method to generate multiple oncolytic HSV vectors and their in vivo evaluation using syngeneic mouse tumor models. Gene Ther. 2006;13(8):705–14. [PubMed: 16421599]

Author Manuscript Author Manuscript Author Manuscript Author Manuscript

17. Wakimoto H, Fulci G, Tyminski E, Chiocca EA. Altered expression of antiviral cytokine mRNAs associated with cyclophosphamide's enhancement of viral oncolysis. Gene Ther. 2004;11(2):214–23. [PubMed: 14712306]
18. Yoo JY, Haseley A, Bratasz A, Chiocca EA, Zhang J, Powell K, et al. Antitumor efficacy of 34.5ENVE: a transcriptionally retargeted and "Vstat120"-expressing oncolytic virus. Mol Ther. 2012;20(2):287–97. [PubMed: 22031239]
19. Haseley A, Boone S, Wojton J, Yu L, Yoo JY, Yu J, et al. Extracellular matrix protein CCN1 limits oncolytic efficacy in glioma. Cancer Res. 2012;72(6):1353–62. [PubMed: 22282654]
20. Thorne AH, Meisen WH, Russell L, Yoo JY, Bolyard CM, Lathia JD, et al. Role of cysteine-rich 61 protein (CCN1) in macrophage-mediated oncolytic herpes simplex virus clearance. Mol Ther. 2014;22(9):1678–87. [PubMed: 24895995]
21. Meisen WH, Wohleb ES, Jaime-Ramirez AC, Bolyard C, Yoo JY, Russell L, et al. The Impact of Macrophage- and Microglia-Secreted TNFalpha on Oncolytic HSV-1 Therapy in the Glioblastoma Tumor Microenvironment. Clin Cancer Res. 2015;21(14):3274–85. [PubMed: 25829396]
22. Hynes RO. Integrins: bidirectional, allosteric signaling machines. Cell. 2002;110(6):673–87. [PubMed: 12297042]
23. Desgrosellier JS, Cheresh DA. Integrins in cancer: biological implications and therapeutic opportunities. Nat Rev Cancer. 2010;10(1):9–22. [PubMed: 20029421]
24. Bai T, Chen CC, Lau LF. Matricellular protein CCN1 activates a proinflammatory genetic program in murine macrophages. J Immunol. 2010;184(6):3223–32. [PubMed: 20164416]
25. You JJ, Yang CH, Yang CM, Chen MS. Cyr61 induces the expression of monocyte chemoattractant protein-1 via the integrin alphanubeta3, FAK, PI3K/Akt, and NF-kappaB pathways in retinal vascular endothelial cells. Cell Signal. 2014;26(1):133–40. [PubMed: 24063814]
26. Digiacomo G, Tusa I, Bacci M, Cipolleschi MG, Dello Sbarba P, Rovida E. Fibronectin induces macrophage migration through a SFK-FAK/CSF-1R pathway. Cell Adh Migr. 2017;11(4):327–37. [PubMed: 27588738]
27. Wang QQ, Li H, Oliver T, Glogauer M, Guo J, He YW. Integrin beta 1 regulates phagosome maturation in macrophages through Rac expression. J Immunol. 2008;180(4):2419–28. [PubMed: 18250451]
28. Tian J, Zhang X, Wu H, Liu C, Li Z, Hu X, et al. Blocking the PI3K/AKT pathway enhances mammalian reovirus replication by repressing IFN-stimulated genes. Front Microbiol. 2015;6:886. [PubMed: 26388843]
29. Dhamanage AS, Thakar MR, Paranjape RS. HIV-1-Mediated Suppression of IFN-alpha Production Is Associated with Inhibition of IRF-7 Translocation and PI3K/akt Pathway in Plasmacytoid Dendritic Cells. AIDS Res Hum Retroviruses. 2018.
30. Xiong Q, Huang H, Wang N, Chen R, Chen N, Han H, et al. Metabolite-Sensing G Protein Coupled Receptor TGR5 Protects Host From Viral Infection Through Amplifying Type I Interferon Responses. Front Immunol. 2018;9:2289. [PubMed: 30333836]
31. Shibue T, Weinberg RA. Integrin beta1-focal adhesion kinase signaling directs the proliferation of metastatic cancer cells disseminated in the lungs. Proc Natl Acad Sci U S A. 2009;106(25):10290–5. [PubMed: 19502425]
32. Cheshenko N, Liu W, Satlin LM, Herold BC. Focal adhesion kinase plays a pivotal role in herpes simplex virus entry. J Biol Chem. 2005;280(35):31116–25. [PubMed: 15994312]
33. Cheshenko N, Del Rosario B, Woda C, Marcellino D, Satlin LM, Herold BC. Herpes simplex virus triggers activation of calcium-signaling pathways. J Cell Biol. 2003;163(2):283–93. [PubMed: 14568989]
34. Holmes KM, Annala M, Chua CY, Dunlap SM, Liu Y, Hugen N, et al. Insulin-like growth factor-binding protein 2-driven glioma progression is prevented by blocking a clinically significant integrin, integrin-linked kinase, and NF-kappaB network. Proc Natl Acad Sci U S A. 2012;109(9):3475–80. [PubMed: 22345562]
35. Chung J, Yoon S, Datta K, Bachelder RE, Mercurio AM. Hypoxia-induced vascular endothelial growth factor transcription and protection from apoptosis are dependent on alpha6beta1 integrin in breast carcinoma cells. Cancer Res. 2004;64(14):4711–6. [PubMed: 15256436]

Author Manuscript Author Manuscript Author Manuscript Author Manuscript

36. Shibue T, Brooks MW, Inan MF, Reinhardt F, Weinberg RA. The outgrowth of micrometastases is enabled by the formation of filopodium-like protrusions. Cancer Discov. 2012;2(8):706–21. [PubMed: 22609699]

37. Jacquemet G, Hamidi H, Ivaska J. Filopodia in cell adhesion, 3D migration and cancer cell invasion. Curr Opin Cell Biol. 2015;36:23–31. [PubMed: 26186729]

38. Fortin S, Le Mercier M, Camby I, Spiegl-Kreinecker S, Berger W, Lefranc F, et al. Galectin-1 is implicated in the protein kinase C epsilon/vimentin-controlled trafficking of integrin-beta1 in glioblastoma cells. Brain Pathol. 2010;20(1):39–49. [PubMed: 18947333]

39. Nam K, Son SH, Oh S, Jeon D, Kim H, Noh DY, et al. Binding of galectin-1 to integrin beta1 potentiates drug resistance by promoting survivin expression in breast cancer cells. Oncotarget. 2017;8(22):35804–23. [PubMed: 28415760]

40. Speicher T, Siegenthaler B, Bogorad RL, Ruppert R, Petzold T, Padrissa-Altes S, et al. Knockdown and knockout of beta1-integrin in hepatocytes impairs liver regeneration through inhibition of growth factor signalling. Nat Commun. 2014;5:3862. [PubMed: 24844558]

41. Jahangiri A, Nguyen A, Chandra A, Sidorov MK, Yagnik G, Rick J, et al. Cross-activating c-Met/beta1 integrin complex drives metastasis and invasive resistance in cancer. Proc Natl Acad Sci U S A. 2017;114(41):E8685–E94. [PubMed: 28973887]

42. Vogelbaum MA, Aghi MK. Convection-enhanced delivery for the treatment of glioblastoma. Neuro Oncol. 2015;17 Suppl 2:ii3–ii8. [PubMed: 25746090]

43. Kalkanis SN. Setting the stage: local delivery of cytoreductive agents for the treatment of glioblastoma. Neuro Oncol. 2015;17 Suppl 2:ii1–ii2. [PubMed: 25746088]

Author Manuscript
Author Manuscript
Author Manuscript
Author Manuscript

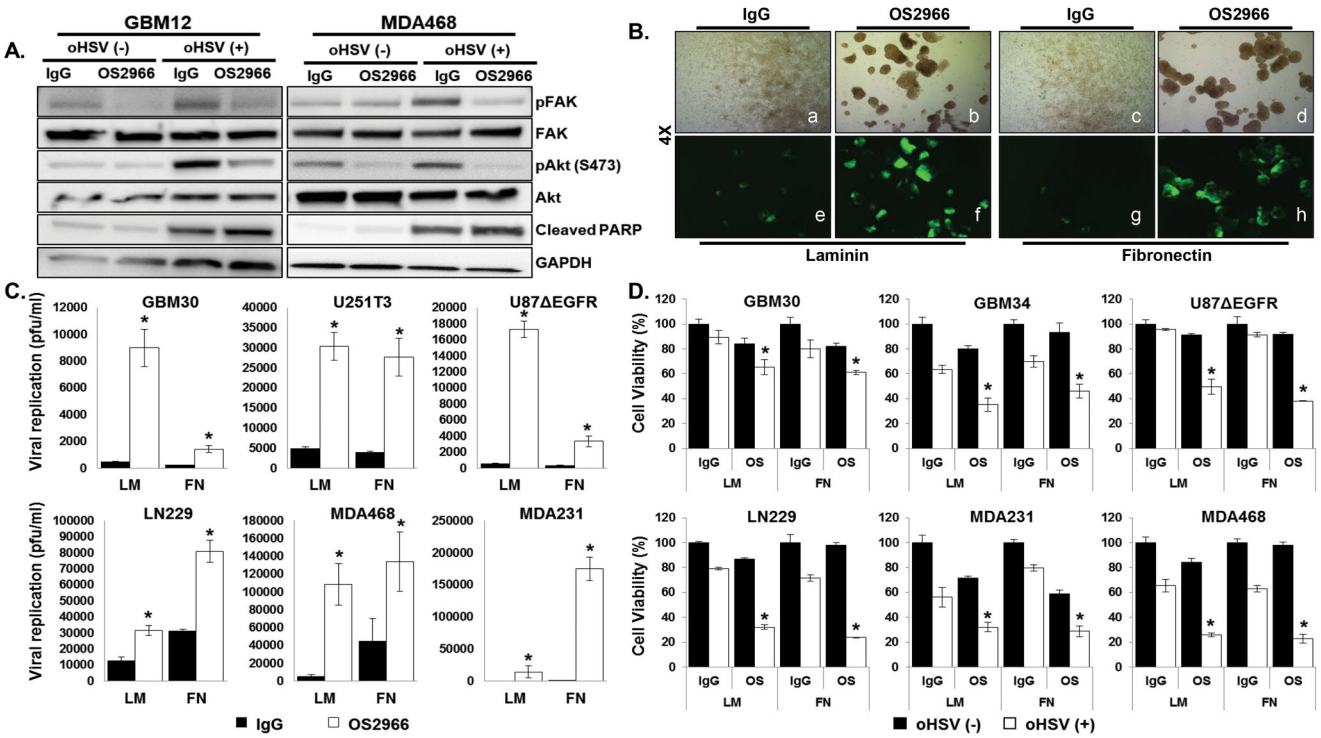

Figure 1. OS2966 treatment inhibits focal adhesion kinase (FAK)-Akt signal pathway and enhances oHSV replication and oHSV-mediated tumor cell killing.

A) patient derived primary GBM (GBM12) and MDA468 breast cancer cells were infected with/without 34.5ENVE (MOI=0.01). Two hours post oHSV infection, unbound viruses were removed and 10 ug/ml of control IgG/OS2966 were added and cultured for 24 hours. Cell lysates were probed with antibodies against phospho-FAK (S397), total FAK, phosphor Akt (S473), total Akt, and cleaved PARP which is downstream of integrin β1-FAK signaling. GAPDH was used as a loading control. **B)** Patient derived primary GBM cells (GBM30) were plated on Laminin (LM)-, or Fibronectin (FN)-coated plates and infected with 34.5ENVE (MOI=0.002). Two hours later, unbound viruses were removed and cultured for 72 hours. Fluorescence microscope images of GFP-positive infected GBM30 cells. **C-D)** The indicated cells were plated on LM-, or FN-coated plates and infected with 34.5ENVE. Two hours later, unbound viruses were removed and cells were treated with 10 μg/ml of control IgG or OS2966. Viral titers were measured by standard plaque forming unit assay (C) and cell viability was measured by MTT assay (D) 72 hours post oHSV infection. *: $p < 0.05$ compared to oHSV + control IgG. *: $p < 0.05$ compared to oHSV + control IgG.

Author Manuscript Author Manuscript Author Manuscript Author Manuscript

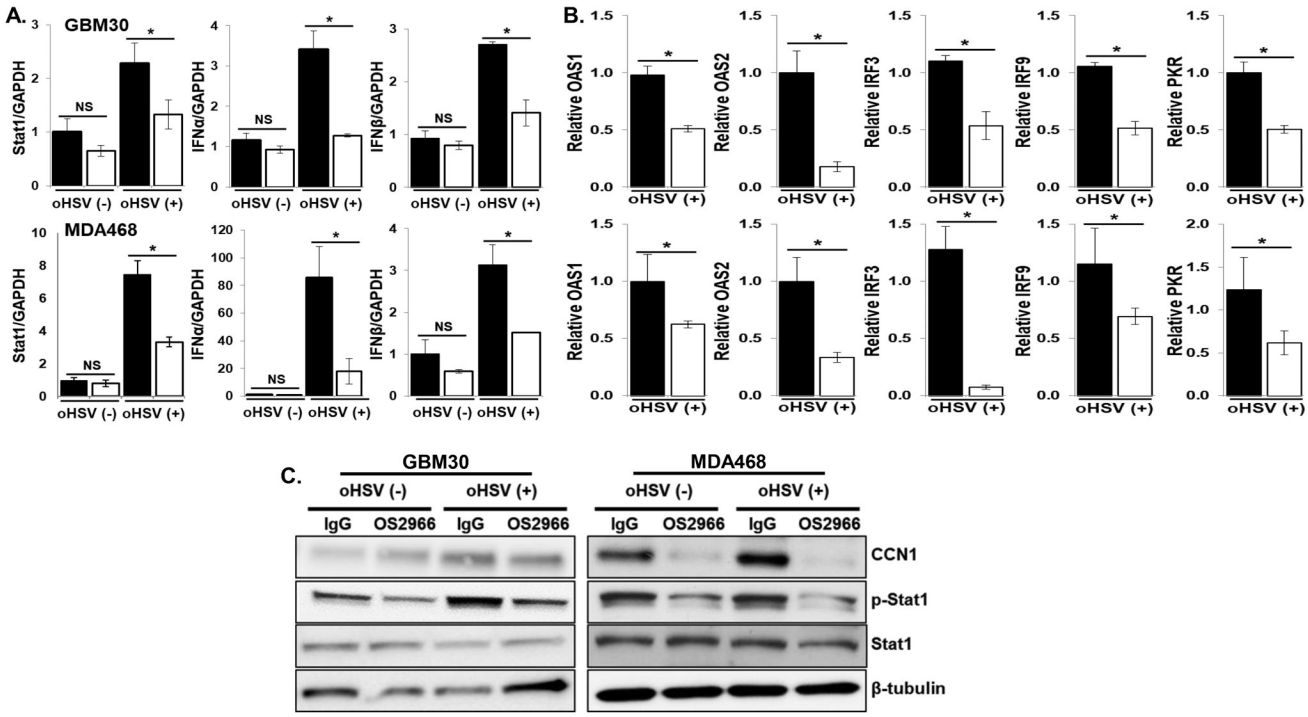

Figure 2. OS2966 inhibits oHSV-mediated anti-viral signaling pathway.

A-B) Impact of OS2966 on oHSV-induced anti-viral signaling. **A)** Real time PCR analysis for changes in gene expression of IFNα, IFNβ, and stat1 gene in both patient derived primary GBM (GBM30) and breast cancer cells 24 hours post oHSV treatment. Data presented are fold changes in gene expression ± SD relative to glyceraldehyde-3-phosphate dehydrogenase (GAPDH). **B)** Real time PCR analysis for changes in a set of the type-I IFN responsive genes involved in the antiviral defense in both patient derived primary GBM (GBM30) and breast cancer cells 24 hours post oHSV treatment. Data presented are relative gene expression between oHSV+OS2966 and oHSV + control IgG. *, $p < 0.05$. Comparisons made between control IgG versus OS2966 and oHSV versus oHSV+OS2966 treated cells. **C)** OS2966 inhibits oHSV-induced CCN1 expression and Stat1 activation. Patient derived primary GBM (GBM30) cells were infected with/without 34.5ENVE (MOI=0.01). Two hours post oHSV infection, unbound viruses were removed and 10 ug/ml of control IgG/OS2966 were added and cultured for 24 hours. Cell lysates were probed with antibodies against CCN1, phosphor-Stat1, and total Stat1. β-tubulin was used as a loading control.

Author Manuscript Author Manuscript Author Manuscript Author Manuscript

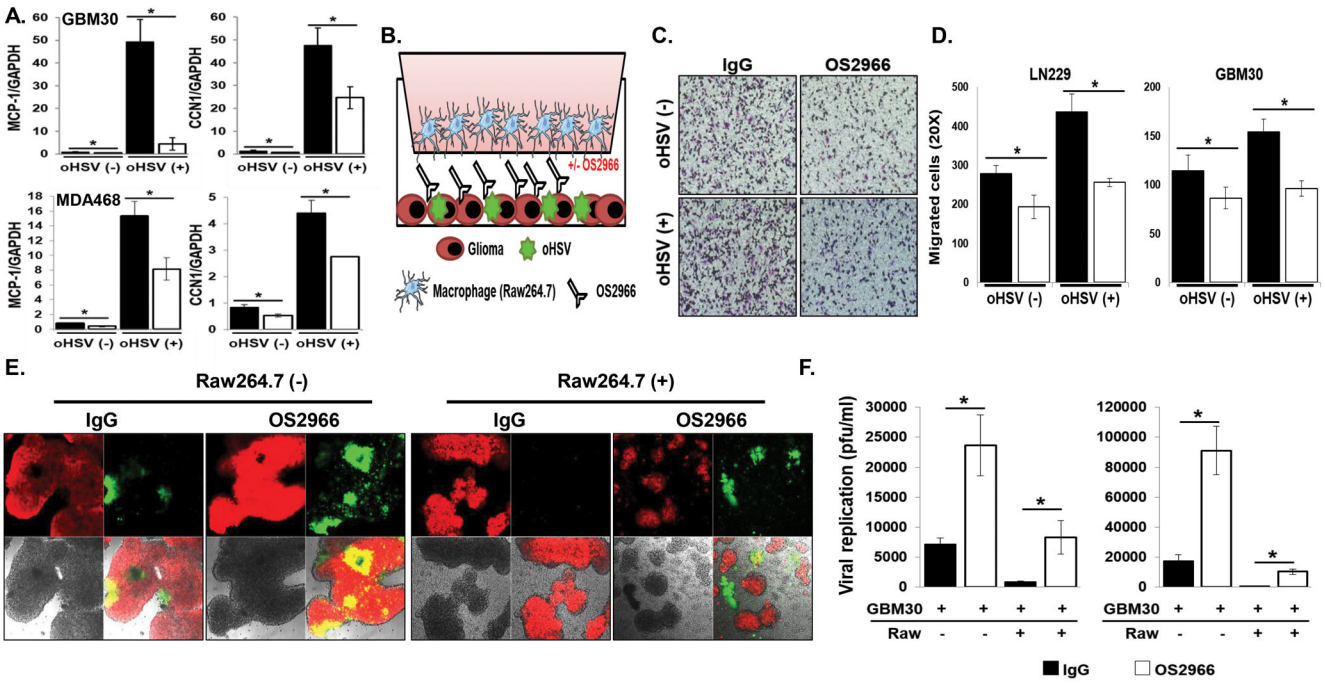

Figure 3. OS2966 inhibits migration of macrophages toward oHSV-infected tumor cells and enhances virus replication in co-culture with macrophages.

A) Real time PCR analysis for changes in gene expression of MCP-1 and CCN1 gene in both patient derived primary GBM (GBM30) and breast cancer cells 24 hours post oHSV treatment. Data presented are fold changes in gene expression ± SD relative to glyceraldehyde-3-phosphate dehydrogenase (GAPDH). **B)** Schematic of macrophage migration assay. **C-D)** LN229 or patient derived primary GBM (GBM12) cells treated with/without 34.5ENVE for 1 hour were treated with 10 ug/ml of IgG or OS2966 and serum starved macrophages were placed in the top chamber. Quantification of migrated Raw264.7 murine macrophages were measured by counting the number of cells that migrated to the bottom side of the transwell membrane 6 hours later. **C)** Representative image of transwell migration assay is shown for each group (×20), respectively. **D)** Quantification of the average number of migrated cells/view field (n = 4/group). Data points represent the mean, and error bars indicate ± SD for each group. **E-F)** Stably mCherry-expressing patient-derived primary GBM cells (GBM30) were treated with oHSV. Two hours post virus infection, unbound viruses were removed and cells were treated with 20 ug/ml of control IgG or OS2966 and then overlaid with serum starved murine macrophage Raw264.7 cells. **E)** Forty-eight hours post co-culture with macrophage, co-culture with oHSV and OS2966 treated cells showed increased GFP-positive, infected cells relative co-culture with oHSV and control IgG treated cells. **F)** Both cells and media were harvested 48 hours after co-culture and viral titers were determined by standard plaque assay. Data points represent the mean, and error bars indicate ± SD for each group. Asterisks indicate statically significant differences between indicated pairs.

Author Manuscript Author Manuscript Author Manuscript Author Manuscript

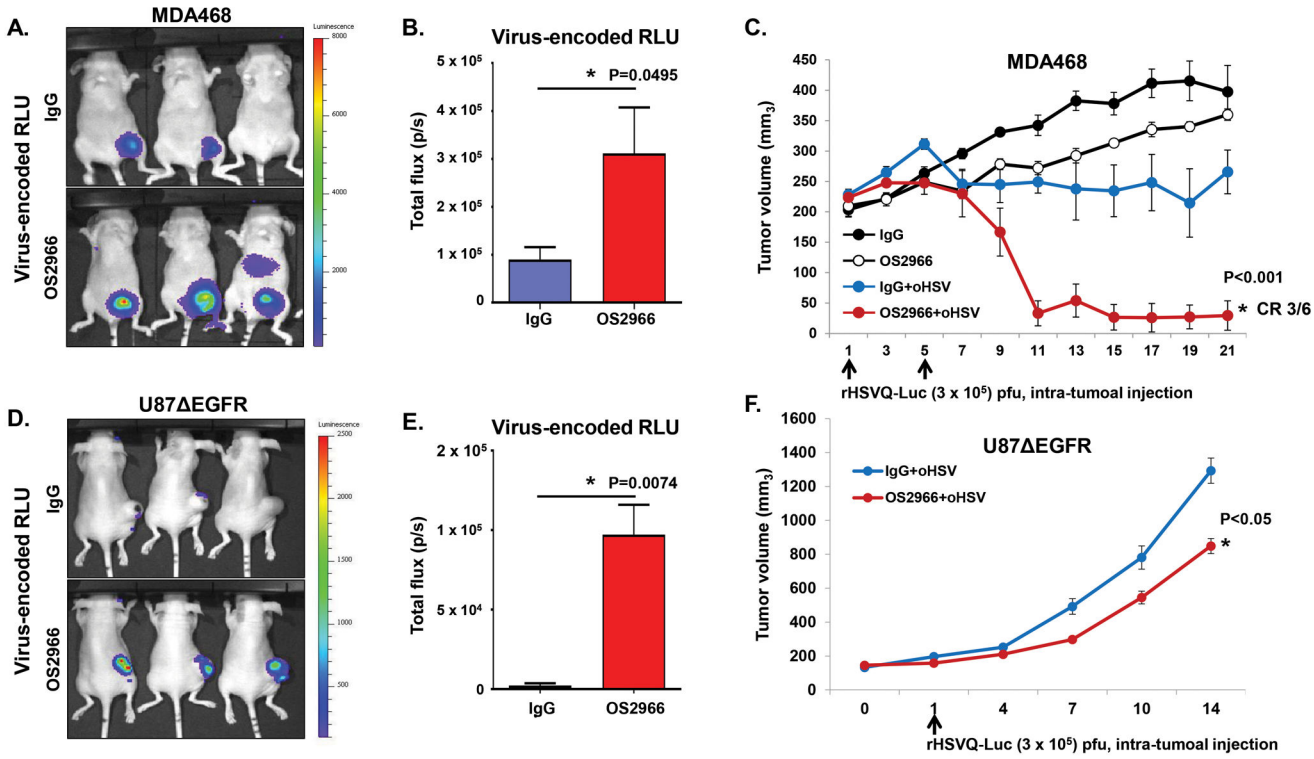

Figure 4. OS2966 treatment increases virus replication and anti-tumor efficacy *in vivo*.

A-C) Athymic nude mice were implanted with MDA468 by mammary fat pad injection. When tumor size reached around 200 mm^3, mice were treated with control IgG or OS2966 (5mg/kg) for 1 day prior to oHSV treatment and twice a week thereafter for the duration of the study, and with 3×10^5 pfu of rHSVQ-Luc on day 1 and 5 (total twice). **A)** Representative luciferase images of oHSV-treated mice with IgG/OS2966 on day 4. **B)** Data shown are total flux in each mouse, indicating quantification of virally expressed luciferase gene activity in MDA468 mammary fat pad injected mice with IgG or OS2966 on day 4. **C)** Tumor volume was measured regularly after treatment and data shown are the mean tumor volumes ± SEM, at the indicated time points (n = 6/group). * indicates $p < 0.05$; rHSVQ-Luc+OS2999 versus rHSVQ-Luc + IgG. **D-F)** Athymic nude mice were subcutaneously implanted with U87ΔEGFR. When tumor size reached around 150 mm^3, 1×10^5 pfu of an oHSV expressing luciferase (rHSVQ-Luc) were injected intratumorally. Control human IgG or OS2966 (5 mg/kg) were administered intraperitoneally on days −1, 1, 3, and 5 after oHSV therapy. **D)** Representative luciferase images of oHSV-treated mice with IgG/OS2966 on day 3. **E)** Data shown are total flux in each mouse treated with IgG or OS2966 on day 3. **F)** Tumor volume was measured regularly after treatment and data points represent the mean of the tumor volumes ± SEM, at the indicated time points (n = 6/group). * indicates $p <$ 0.05; rHSVQ-Luc+OS2999 versus rHSVQ-Luc + IgG.

Author Manuscript Author Manuscript Author Manuscript Author Manuscript

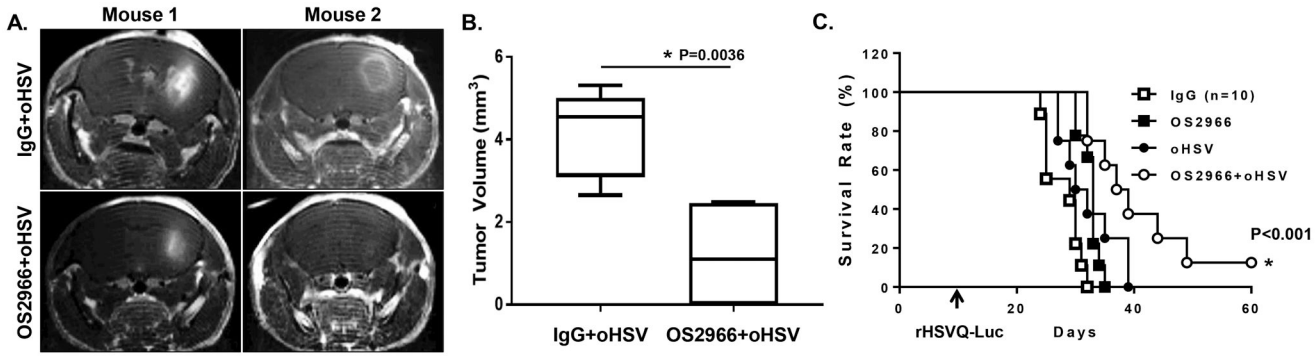

Figure 5. Combination treatment with oHSV and S2966 enhances survival of patient derived primary GBM (GBM12)-bearing mice *in vivo*.

A-C) Athymic nude mice bearing intracranial patient derived primary GBM12 tumors were treated with control IgG or OS2966 (5mg/kg) intra-tumorally twice a week for 1 month. oHSV were injected by IT injection on day 10 after tumor implantation and mice were then monitored for survival. (A) T1-weighted MRI images of coronal sections of tumor-bearing mice 3 days post oHSV treatment (13 days post tumor implantation). (B) The volume of tumor measured on MRI. (C) Data shown are Kaplan-Meier survival curves of animals in each group (n=8 for IgG, OS2966, and oHSV+IgG, and oHSV+OS2966). Mice were euthanized when they showed symptoms of hunched posture, rough coat, thin body, or limb paralysis.